ELSEVIER

Journal of Power Sources 112 (2002) 290–293

JOURNAL OF POWER SOURCES

www.elsevier.com/locate/jpowsour

Improvement in the electrochemical performance of $Li_xV_2O_5$ induced by Tb doping

E.C. Almeida[a], M. Abbate[b], J.M. Rosolen[a,*]

[a]*Departamento de Química, FFCLRP-USP, 14040-901 Ribeirão Preto SP, Brazil*
[b]*Departamento de Física, UFPR, Caixa Postal 19091, 81531-990 Curitiba PR, Brazil*

Received 12 July 2002; accepted 19 July 2002

Abstract

We have studied the electrochemical behavior of $Tb_{0.11}V_2O_5$ electrodes in propylene carbonate and $LiClO_4$. The techniques used in the study were cyclic voltammetry, discharge/charge polarization, FTIR and XRD. The $Tb_{0.11}V_2O_5$ compound was prepared using the xerogel route and the composite electrodes were membranes prepared with PVDF-binder and carbon. The results show that the Tb doping improves the electrochemical performance of V_2O_5 due to the bonding of the earth-rare ions and the residual H_2O in the V_2O_5 structure. The capacity fading was reduced, the specific reversible capacity was 330 mA g^{-1} (C/4, cut-off 3.7–2.0 V) and the voltage presented a large plateau at 2.5 V for the $Tb_{0.11}V_2O_5$ electrodes. The charge transfer between Li and $Tb_{0.11}V_2O_5$ does not involve the oxidation–reduction of the Tb^{3+} ions.

Keywords: Vanadium oxide; Rare-earth; Battery

1. Introduction

The specific capacity and the capacity fading of V_2O_5 electrodes depend strongly on structural characteristics. For example, it is known that amorphous V_2O_5 xerogel (xrg) has higher capacities for Li insertion than crystalline c-V_2O_5. It has been reported that xrg-V_2O_5 are able to intercalate 1.6 equivalent Li/mol V_2O_5, while the c-V_2O_5 is able to intercalate only 0.78 equivalent Li/mol V_2O_5 [1–5]. However, the capacity fading of xrg-V_2O_5 composite electrodes is much larger than that found for c-V_2O_5 (although its amorphous structure appears better suited to support the stress produced by the Li intercalation).

The H_2O in the xrg-V_2O_5 tends to bind to unreacted species and decreases the mobility of the Li ions. In fact, a recent XAS study of a $Li_xV_2O_5$ xerogel detected the reaction with H_2O with the formation of Li_2O [6]. Improvements of the capacity fading and specific capacity of xrg-V_2O_5 was achieved by Cu and Ag doping [7] (it is believed that the extra ions bind to the H_2O in the structure increasing the mobility of the intercalated Li ions). XAS studies of $Li_xCu_{0.1}V_2O_5$ demonstrated that the Cu ions exchange charge with the Li ions and are reduced [8].

Here, we report the changes in the electrochemical response of a crystalline V_2O_5 xerogel doped with Tb (this lanthanide was chosen because it has only one possible oxidation state Tb^{3+} at room temperature). The main characterization techniques were FTIR, XRD, cyclic voltammetry, and galvanostatic charge-discharge. It was found that the reversible specific capacity of the rare-earth doped xrg-V_2O_5 is greatly improved. This improvement is attributed to the bonding of the rare-earth ions to the residual H_2O in the xerogel structure.

2. Experimental details

The vanadium pentoxides xerogels (xrg) studied in this work were prepared by the sol–gel route. The hydrogels were synthesized utilizing a 0.5 M sodium metavanadate solution (Alfa) and a proton exchange resin (Bayer, Lewatit S 100). The V_2O_5 doped with Tb was prepared by mixing stoichiometric quantities of $Tb(OH)CO_3$ hydrated to yellow HVO_3 solution (0.5 M). The $Tb(OH)CO_3$ hydrated precursor was obtained from a reaction between Tb_2O_3, urea and $NH_4(OH)$ (after centrifugation at $T = 60\,^{\circ}C$). The high solubility of $Tb(OH)CO_3$ in acid pH guarantees a complete ionic exchange reaction between the cationic species Tb^{3+} and HVO_3 (the reaction products are $Tb_{0.11}V_2O_5{\cdot}nH_2O$ and CO_2). The resulting hydrogels (red solution) were aged for 8

* Corresponding author. Tel.: +55-16-602-3787; fax: +55-16-633-8151.
E-mail address: rosolen@ffclrp.usp.br (J.M. Rosolen).

0378-7753/02/$ – see front matter
PII: S0378-7753(02)00448-2

days and then heated at 50 °C for 12 h becoming a powder. The resulting xerogels were then heated at 300 °C for 4 h in a vacuum of 0.9 bar. The powders were then milled using a mortar and then sieved (300 mesh) in atmosphere and stored in a dry-box (Mbraum) before any use.

Composite electrodes were prepared with 10% polyvinylidene fluoride PVDF (Solvay), 10% carbon (ketjen black, MMB) and 80% xerogel (V_2O_5 or $Tb_{0.11}V_2O_5$). The xerogel and carbon were mixed in a mortar and afterwards added to the binder solution (PVDF dissolved in acetone). The slurry obtained was spread on a glass using a doctor blade. The membrane obtained was cut in the form of disks (8 mm in diameter). The electrochemical characterizations were performed in a coin cell where lithium was used both as the auxiliary and reference electrodes. The material used in the current collectors of the coin cell type was stainless steel. Two layers of separator (Celgard) were used in the electrochemical cells. The electrolyte was a 1 mol l^{-1} $LiClO_4$ (Aldrich, dried at 120 °C in a vacuum) in propylene carbonate (Aldrich). All the membrane electrodes were dried in a vacuum of 0.9 bar at 70 °C for 4 h before the assembly of the cell in the dry-box.

Galvanostatic charge/discharge cycles were performed using a Mac-Pile cycler, while the linear sweep voltammetry experiments were carried out with a PAR-362 using Labview. The powder XRD diagrams were collected using a Phillips 2001 diffractometer (Cu Kα radiation, graphite monochromator, range 10–90°, steps of 0.02°, and 3 s/step). The FTIR spectra were collected using a Nicolet 5ZDX spectrometer (KBr beam splitter, 64 acquisitions, resolution 2 cm^{-1}, and transmission mode).

3. Results and discussion

Fig. 1 shows the FTIR spectra and XRD patterns of the $Tb_{0.11}V_2O_5$ and V_2O_5 xerogels. The thermal treatment applied during the preparation resulted in the crystallization of both materials. The XRD patterns of xrg-V_2O_5 and xrg-$Tb_{0.11}V_2O_5$ present features of polycrystalline orthorhombic V_2O_5. This similarity with polycrystalline V_2O_5 indicates that the Tb ions occupy interstitial sites between the VO_6 layers. However, the reduced intensity in the XRD diagram of xrg-$Tb_{0.11}V_2O_5$ suggests that it is less crystalline than xrg-V_2O_5. This is also supported because some of the reflections are not even observed in the pattern of xrg-$Tb_{0.11}V_2O_5$. The resulting interplanar d_{001} spacing of xrg-V_2O_5 was around 4.45 Å, while for xrg-$Tb_{0.11}V_2O_5$ it was about 4.41 Å.

The local order of the V_2O_5 xerogel probed by FTIR is also modified upon Tb^{+3} insertion. The FTIR spectra present bands from 950 to 1020 cm^{-1} that correspond to the V–O vanadyl stretching modes, while the bands between 700 and 900 cm^{-1} can be ascribed to the bending V–O–V modes. The bands below 600 cm^{-1} could be due either to edge-sharing 3V–O stretching or bending V–O–V deformations. The main differences observed in the FTIR spectra are the shift of the 3V–O (around 531 and 592 cm^{-1}) and V–O bands (about 1016 and 1020 cm^{-1}). The displacement of these bands are associated with structural alterations caused by changes in the ionic force of the V–O. The presence of the small shoulder about 980cm^{-1} in V_2O_5 confirms that this xerogel is more crystalline than $Tb_{0.11}V_2O_5$.

The XRD and FTIR results reflect the concentration of interlayer H_2O in the xerogels and the interaction bewteen Tb^{3+} and H_2O. TGA/DTAdifferential thermal analysis performed in N_2 showed that the H_2O concentration in $Tb_{0.11}V_2O_5.nH_2O$ was 0.1 moles, while in $V_2O_5{\cdot}nH_2O$ the n value was 0.5 moles. However, the XRD patterns and the FTIR spectra indicated that the V_2O_5 xerogel was more crystalline than $Tb_{0.11}V_2O_5$. This difference in the $Tb_{0.11}V_2O_5$ compound is attributed to a interaction between the Tb^{3+} ions and H_2O (possibly the so called lanthanide contraction that affects the interaction between H_2O and the VO_6 layers).

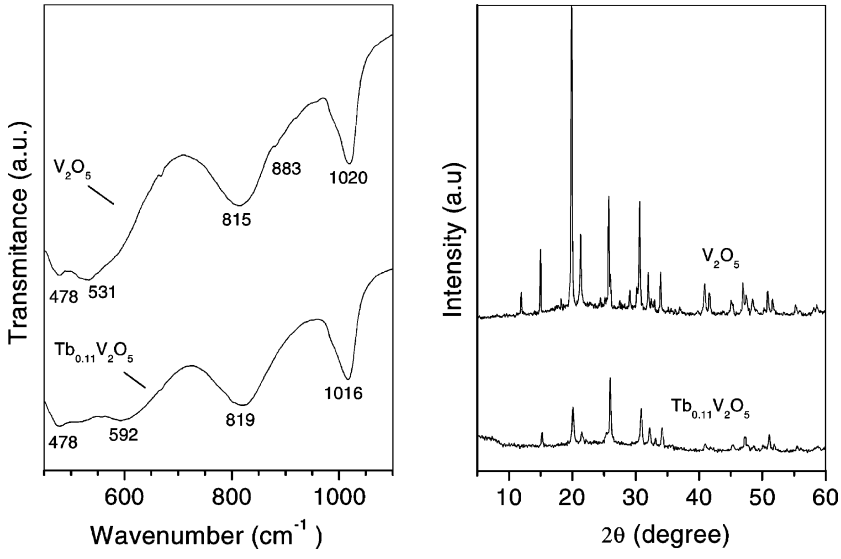

Fig. 1. XRD diagrams and FTIR spectra of V_2O_5 and $Tb_{0.11}V_2O_5$ xerogels.

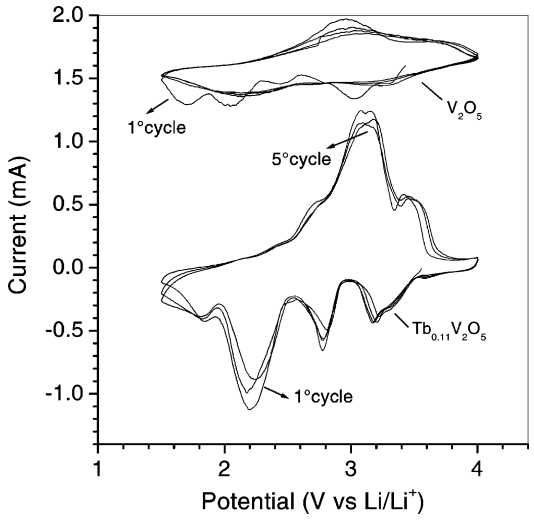

Fig. 2. Cyclic voltammogram of composite electrodes prepared with V_2O_5 and $Tb_{0.11}V_2O_5$ xerogels.

Fig. 2 shows the voltammetric curves of composite electrodes prepared with V_2O_5 and $Tb_{0.11}V_2O_5$ xerogels (the voltammogram of V_2O_5 was shifted up by 1.6 mA). The voltammograms were performed in the scanning range 3.9–1.5 V (scan-rate 0.1 mV s^{-1}) and exhibit clear differences. The peak currents of the $Tb_{0.11}V_2O_5$ electrode were more intense than those found for the V_2O_5 electrode. Further, the voltammogram of the $Tb_{0.11}V_2O_5$ electrode was more stable upon repeated charge/discharge cycles. The peaks and shoulders of the $Tb_{0.11}V_2O_5$ voltammogram remained practically the same, whereas for the V_2O_5 voltammogram the peaks and shoulders observed during the first cathodic scan changed completely. Finally, the peaks in $Tb_{0.11}V_2O_5$ appear displaced to higher values than those found in V_2O_5 during the first cycle.

The peaks in the voltammograms of lithium intercalation electrodes are associated with different lithium occupation sites. Alterations in the position and profile of the peaks can be thus correlated to structural modifications in the host. The voltammograms of Fig. 2 present four cathodic peaks for both electrodes during the first cathodic scan. When the scan is inverted in the anodic direction, the V_2O_5 curve had two supperimposed anodic peaks, while the $Tb_{0.11}V_2O_5$ voltammogram exhibits four peaks that are superposed in the potential range 2.4–4 V (one small shoulder is also visible at about 2.3 V). Therefore, the first insertion of lithium in $Tb_{0.11}V_2O_5$, until 1.5 V, does not induce any structural changes, whereas clear irreversible changes are observed in the V_2O_5 case.

Fig. 2 suggests that the insertion of Tb in the V_2O_5 structure improves its electrochemical performance. The composite electrode $Tb_{0.11}V_2O_5$ presents not only a better structural stability, but also better kinetics for lithium intercalation. The peak currents for $Tb_{0.11}V_2O_5$ have much larger values and the superposition of peaks is smaller than in V_2O_5. The improvement in the lithium diffusion may be associated with a possible increase of electronic conductivity in $Tb_{0.11}V_2O_5$. The Tb^{3+} ions does not seem to participate of oxidation–reduction process associated with reversible intercalation of lithium (Tb^{2+} is impossible and Tb^{4+}). Thus, the peaks of voltammograms for both xerogels are associated with the occupation of lithium and the oxidation–reduction of V or O ions. Finally, it is important to notice again that for the $Tb_{0.11}V_2O_5$ compound, the first lithium insertion does not induce an irreversible structural modification like that observed in V_2O_5. For polycrystalline orthorhombic V_2O_5, the irreversible structural alterations are attributed to phase transition and/or phase segregation that reduces the specific capacity when the intercalation goes beyond $x = 1$ in $Li_xV_2O_5$ [9].

Fig. 3 shows the specific capacity of the $Tb_{0.11}V_2O_5$ composite electrode versus discharge/charge cycle (see the inset), as well as its voltage response versus lithium concentration compared with the V_2O_5 composite electrode for low current density (0.01 mA cm^{-2}). The profile of the voltage curve is typical of crystalline compounds and, as expected, has several plateaux that occur in the same potentials of cathodic peaks detected in the first discharge of voltammograms. The potential curve is related to the chemical potential of the ions and electrons and, for amorphous xerogels, it does not contain any plateaux [1]. The voltage curve of Fig. 3 reveals that the structural effects provoked by the Tb insertion into the polycrystalline xerogel affects mostly the beginning of the insertion (for $x > 0.1$, in $Li_xV_2O_5$ and $Li_xTb_{0.11}V_2O_5$). The curve of the composite

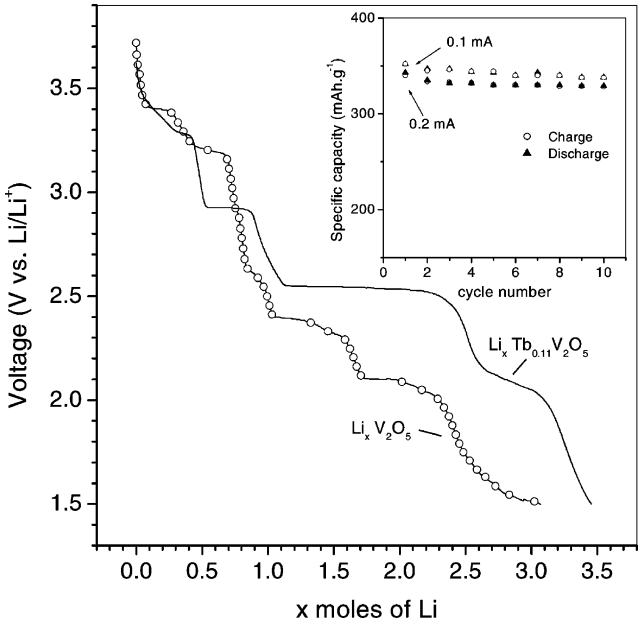

Fig. 3. Variation of the voltage with the lithium concentration of composite electrodes prepared with V_2O_5 and $Tb_{0.11}V_2O_5$ xerogels (discharge current 0.01 mA cm^{-2}). The inset gives the specific capacity of the $Tb_{0.11}V_2O_5$ composite electrode vs. cycle number at 0.1 mA and 0.2 mA (area of the electrode 0.502 cm^2).

electrode prepared with $Tb_{0.11}V_2O_5$ for $0.5 < x < 2.7$ has more extended plateaux than that of the V_2O_5 electrode (further, these plateaux appear at higher potential). The evolution of the specific capacity of the $Tb_{0.11}V_2O_5$ electrode confirms its good structural stability (see Fig. 3), which was also suggested by the low scan rate voltammograms (see Fig. 2). For a discharge/charge current equal to 0.2 mA, the specific capacity in the tenth discharge/charge cycle (cut-off 3.7–2.0 V) were 330 mA g^{-1} (C/4) and 119 mA g^{-1} (C/10) for $Tb_{0.11}V_2O_5$ and V_2O_5, respectively.

Therefore, the $Tb_{0.11}V_2O_5$ electrode has a better lithium intercalation kinetic and structural stability then V_2O_5 composite electrode. Both vanadium pentoxide xerogels studied here are polycrystalline compounds, but they contain H_2O molecules. In fact, the H_2O molecules had a fundamental role in the electrochemical performance of our materials. We have also studied composite electrodes prepared with $Tb_{0.11}V_2O_5$ and V_2O_5 powders submitted to a second thermal treatment (heating at 300 °C for 4 h and another 1 h in 400 °C in a vacuum of 0.1 bar) to completely extract all the H_2O. For the later compounds, the improving of the electrochemical response obtained after Tb insertion was less important. In fact, the $Tb_{0.11}V_2O_5$ compound completely free of water had a very poor capacity and cyclic behavior cut-off (1.5−3.9 V or 2.0−3.9 V) [10]. Thus, the interaction between Tb and H_2O molecules seems to be responsible for the enhancement of the electrochemical performance of the polycrystalline V_2O_5 xerogel. The Tb^{3+} ions must be hydrolyzed into V_2O_5 xerogel structure $(Tb(H_2O)_n)^{3+}$ in aqueous solution), this hydrolysis may affect the polarization of the first hydration sphere, polarization that increases with the shrinking of the lanthanide size. The intercalation charge in the polycrystalline $Tb_{0.11}V_2O_5$ is largely associated with the vanadium cation and/or oxygen, which is different from that observed for unpillared vanadium pentoxide $Cu_{0.1}V_2O_5$ [7]. The Tb^{3+} does not participate of the oxidation–reduction process during the intercalation of lithium, and it did not alter the charge of vanadium and oxygen because of its bonding with H_2O molecules. A recent XAS study of Li_x $Eu_{0.11}V_2O_5$ has demonstrated that the electronic structure of V_2O_5 is not drastically affected by Eu doping and Li_2O can be formed during lithium insertion [10].

4. Conclusions

We studied the influence of Tb doping in polycrystalline V_2O_5 obtained by the sol–gel route. The Tb doping was carried out in the hydrogel using $Tb(OH)CO_3$. The Tb provoked an improvement of the lithium intercalation kinetic and structural stability of V_2O_5. The composite electrodes prepared with $Tb_{0.11}V_2O_5$ presented a specific capacity of 330 mA g^{-1} for a cut-off of 3.7–2.0 V, and exhibits a lwgel plateau at about 2.55 V versus Lithium. The electrochemical improvement was attributed to bonding between the earth-rare ions and the residual H_2O in the V_2O_5 structure. The charge transfer between Li and $Tb_{0.11}V_2O_5$ does not involve the oxidation–reduction of the Tb^{3+} ions. Therefore, $Tb_{0.11}V_2O_5$ compound appears attractive for its uses in lithium intercalation devices.

Acknowledgements

This work was supported by CNPq-PADCT (620238/97-6), PRONEX and Fundação Araucaria. The authors are grateful to Prof. O.A. Serra for stimulating discussions and helpful support.

References

[1] B.B. Owens, S. Passerini, W.H. Smyrl, Electrochim. Acta 45 (1999) 215–224.
[2] K. West, B. Zachauchristiansen, T. Jacobsen, S. Skaarup, Electrochim. Acta 38 (1993) 1215–1219.
[3] H.K. Park, W.H. Smyrl, J. Electrochem. Soc. 141 (1994) L25.
[4] H.K. Park, W.H. Smyrl, M.D. Ward, J. Electrochem. Soc. 142 (1995) 1068–1072.
[5] A.L. Tipton, S. Passerini, B.B. Owens, W.H. Smyrl, J. Electrochem. Soc. 143 (1996) 3473–3476.
[6] E.C. Almeida, M. Abbate, J.M. Rosolen, Solid State Ionics 140 (2001) 241–248.
[7] F. Coustier, G. Jarero, S. Passerini, W.H. Smyrl, J. Power Sources 83 (1999) 9–14.
[8] M. Giorgetti, S. Mukerjee, S. Passerini, J. McBreen, W.H. Smyrl, J. Electrochem. Soc. 148 (2001) A778.
[9] B. Pecquenard, D. Gourier, N. Baffier, Solid State Ionics 78 (1995) 287–303.
[10] E.C. Almeida, Master Thesis, FFCLRP-USP (2001).